RADIO AND X-RAY IMAGES OF RADIO GALAXY AND QUASAR JETS GENERATED BY MOVING SOURCE OF RELATIVISTIC ELECTRON INJECTION

E. Yu. Bannikova
Institute of Astronomy of Kharkiv National University
4 Svobody Sqr., 61077 Kharkov, Ukraine
BANNIKOVA@ASTRON.KHARKOV.UA
V. M. Kontorovich
Institute of Radio Astronomy of the National Academy of Science of Ukraine
4 Chervonopraporna Str., 61002 Kharkov, Ukraine
VKONT@IRA.KHARKOV.UA

Abstract

The similarity and difference between the images of jets of extragalactic sources in radio and X-ray bands, created by the same distribution of relativistic electrons due to synchrotron (for radio) and inverse Compton scattering (for X-ray) is discussed. We restrict ourselves to the vicinity of the moving sources of relativistic electrons — jet knots and hot spots — with diffusion as the spreading mechanism of the electrons. The case of independence on coordinates purely Compton losses on relic radiation is considered. The form of "flares" near jet knots is investigated. It is shown, that the heterogeneity of a magnetic field can result in characteristic differences in the form and location of radio and X-ray isophotes depending whether the magnetic field decreases or increases to the periphery of the source.

1 Introduction

In some radio galaxies there are radio and X-ray jets with local knots (Kn) and hot spots (HS)[1]. They often have fine structure in the form of asymmetric "flares", that may be a result of movement of Kn or HS. The way of getting physical parameter combinations (such as a magnetic field strength, jet or knot velocity, etc.) is offered by investigating these "flares".

[1] See Harris' list of radio sources with jet related X-ray emission http://hea-www.harvard.edu/XJET/

2 Diffusion model with a moving knot or hot spot

In this paper the HS or Kn are considered as localized moving sources of ultra relativistic electrons further propagating into a cloud or jet where they lose their energy for synchrotron and/or Compton radiation. The input equation is the kinetic equation (KE) for the electron distribution function (EDF), $N(E,t,\mathbf{r})$, with a given moving source, where $Q = Q(E,t,\mathbf{r})$, and with diffusion as a mode of electron propagation (Ginsburg, 1984; Valtaoja, 1982; Gestrin, Kontorovich & Kochanov, 1987; Kolesnikov & Kontorovich, 2001; Bannikova & Kontorovich, 2003a):

$$\frac{\partial N}{\partial t} + \frac{\partial (B(E)N)}{\partial E} - D(E)\triangle N = Q(E,t,\mathbf{r}), \quad (1)$$

where

$$\triangle \equiv \frac{\partial^2}{\partial x^2} + \frac{\partial^2}{\partial y^2} + \frac{\partial^2}{\partial z^2}.$$

The second term in KE describes the Compton losses of an electron

$$B(E) = -\beta E^2,$$

$$\beta = \frac{32\pi}{9}\left(\frac{e^2}{mc^2}\right)^2 \frac{W_r}{m^2c^3},$$

where e is the electron charge, m is the electron mass, c is the velocity of light, and W_r denotes the energy density of radiation. In this work we assume that the diffusion factor is a constant value ($D \equiv D_0$). By making a change of variables in the $t-E$ plane (or Laplace

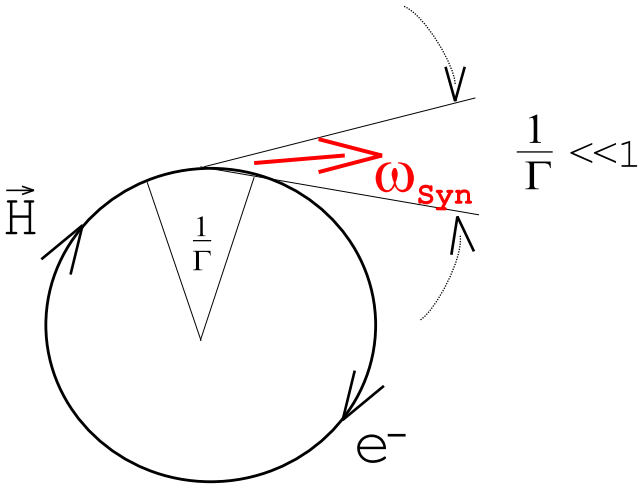

Figure 1: Schematic of synchrotron radiation.

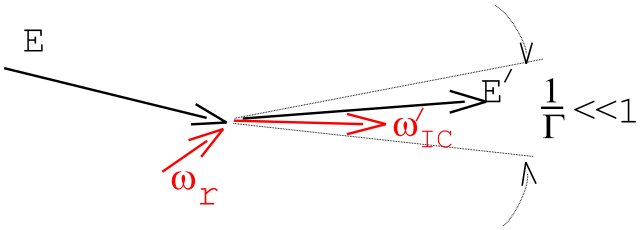

Figure 2: Schematic of inverse Compton scattering.

transformation in time) we can reduce the KE (in terms of a new variables) in the case of a space-uniform decay to a diffusion equation which has a known solution. The final expression for the EDF with a moving (point) source located at **r(t)** $= [x(t), y(t), z(t)]$, where x and y are coordinates in a picture plane, is given by

$$N(E,t,\mathbf{r}) = \frac{Q_0}{(4\cdot\pi)^{3/2}\cdot E^2}\int\limits_{-\tau_+}^{\tau_-}\frac{d\tau'_-}{\alpha^{3/2}(\tau_+,\tau_-,\tau'_-)}\times$$
$$\times(\tilde{E}(\tau_+,\tau'_-))^{-\gamma_0+2}\times$$
$$\times\Theta(E_2-\tilde{E}(\tau_+,\tau'_-))\cdot\Theta(\tilde{E}(\tau_+,\tau'_-)-E_1)\times$$
$$\times\exp\left(-\frac{(x-x(\tau_++\tau'_-))^2+(y-y(\tau_++\tau'_-))^2+(z-z(\tau_++\tau'_-))^2}{4\alpha(\tau_+,\tau_-,\tau'_-)}\right), \quad (2)$$

with

$$\alpha(\tau_+(E,t),\tau_-(E,t),\tau'_-) = \int\limits_{\tau'_-}^{\tau_-(E,t)} d\tau_2 D(\tau_+(E,t),\tau_2),$$

$$\tilde{E}(\tau_+(E,t),\tau'_-) = \frac{1}{\frac{1}{E_2}-\beta\cdot(\tau_+(E,t)-\tau'_-)},$$

$$\tau_+(E,t) = \frac{1}{2\beta}\left(\beta\cdot t+\frac{1}{E_2}-\frac{1}{E}\right),$$

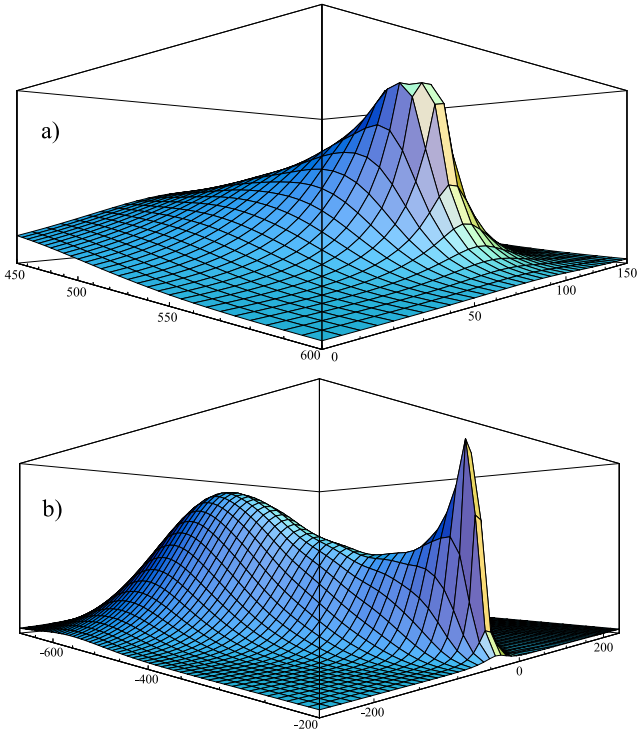

Figure 3: The electron distribution function with parameters according to a) the model image in Fig. 5a (uniform field); b) the model image in Fig. 6c (asymmetric nonuniform field).

$$\tau_-(E,t) = \frac{1}{2\beta}\left(\frac{\beta\cdot t}{2}\frac{1}{E_2}+\frac{1}{E}\right),$$

where $\Theta(...)$ is Havyside's step function and E is the electron energy. Knowing the EDF (Fig. 3) it is possible to find the intensity both of the synchrotron radiation and radiation due to the inverse Compton effect.

The intensity distribution of synchrotron, I_s, (Landau & Lifshits, 1988) and Compton, I_C, (Zheleznyakov, 1997) radiation for the sources resolved by a radio telescope (such as the Very Large Array) or by a modern space X-ray telescope (*Chandra*) is equal to

$$I_s(\nu,t,\mathbf{r}) = \frac{\sqrt{3}e^3}{mc^2}\int^{E_2} dE\int dz\cdot N(E,t,\mathbf{r})\times$$
$$\times H\frac{\nu}{\nu_s}\int_{\nu/\nu_s}^{\infty} K_{5/3}(\eta)\cdot d\eta \quad (3)$$

$$I_C(\nu,t,\mathbf{r}) = hc\nu\int dz\int_0^{\infty} dE\int_{h\nu}^{\infty}\sigma(\epsilon,E)\times$$
$$\times n_{ph}(\epsilon)N(E,t,\mathbf{r})d\epsilon \quad (4)$$

$$\nu_s = \nu_H\left(\frac{E}{mc^2}\right)^2, \qquad \nu_C = \nu_{ph}\left(\frac{E}{mc^2}\right)^2,$$

where $\nu_H = 3eH/(4\pi mc)$, H is the magnetic field projection on the image plane, $\int dz$ is an integral along the line of sight, $K_{5/3}$ is the modified Bessel function,

$\sigma(\epsilon, E)$ is the cross-section of the Compton scattering, and $n_{ph}(\epsilon)$ is the low frequency photon distribution with typical frequency ν_{ph} for one of the scattering processes on the relic radiation. We consider only the transparent region. The injection spectrum is supposed to follow the power law ($E^{-\gamma_0}$) with $\gamma_0 = 2$ in the range of energies $E_1 < E < E_2$, and to be equal to zero outside. Characteristic frequencies which correspond to lower and upper limits by energy have been chosen starting from the condition: $\nu_s(E_1) \ll \nu \ll \nu_s(E_2)$ for the radio band and $\nu_C(E_1) \ll \nu \ll \nu_C(E_2)$ for the X-ray band, where ν is frequency for which the intensity maps have been calculated. The injection is switched on at time $t = 0$ which corresponds to the beginning of effective particle acceleration.

Thus, if we know the EDF ($N(E, t, \mathbf{r})$) and use Eq. (3) and/or Eq. (4), it is possible to build maps of intensity distributions. Since the intensity of radiation of an individual electron (the multiplier to the right of the magnetic field in Eq. (3)) is a sharp function of frequency, we have replaced it by the delta-function to simplify the calculations, i.e., we have considered $\nu \simeq \nu_s$. The numerical calculations were made in the `Mathematica 5.0` package using the double exponential convergence algorithm.

The parameters we find are the life time of the electron with energy E, $\tau \approx 1/(\beta E)$; the diffusion length, $\lambda_{\rm dif} \cong \sqrt{D_0 \tau}$, and the diffusion velocity, $V_{\rm dif} = \sqrt{D_0/\tau}$, which is the ratio of the longitudinal velocity V and the transverse velocity of HS or Kn governs the cloud geometry at a given frequency (Fig. 4). Using geometric considerations the relative velocity can be estimated as $V \approx \beta E\,(L - l)$. We attempt to obtain a similarity between model and observed images by varying parameters. For a qualitative analysis and preliminary estimations geometrical relations are used.

We have received the maps of flare intensity distribution and compared these with observational data for the jet knots *A* and *B* of the radio galaxy M87, for the southern jet component of the microquasar 1E1740.7−2942 in the Galactic center, and also for the parsec scale jet of NGC4261 (Bannikova & Kontorovich, 2003a). In the latter case the diffusion perhaps has to be replaced by a flow[2].

[2]This does not essentially change the nature of the problem, viz. a local source (HS or Kn), the electron propagating away from it and undergoing the synchrotron-Compton losses. But the form of the flare starts depending on additional parameters. The account of flow is essential at low frequencies far from the source of electrons

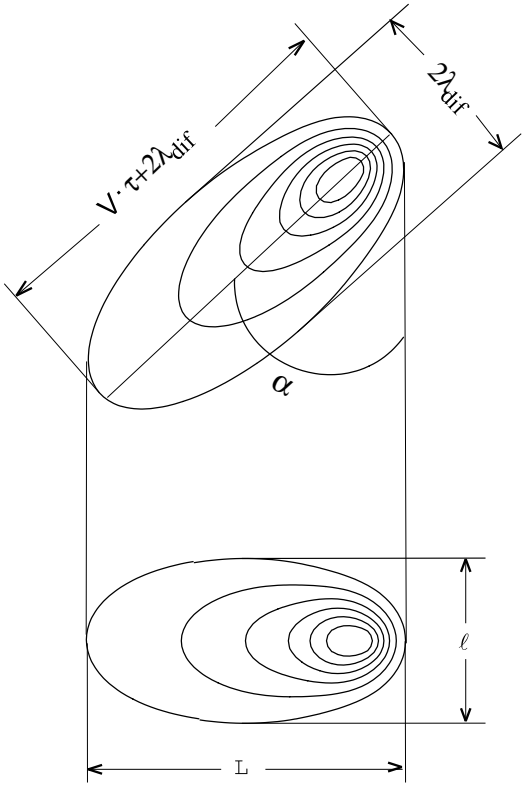

Figure 4: Schematic "flare" which moves by an angle α with respect to the line of sight.

3 Influence of inhomogeneous magnetic field on source images

It is essential that relativistic electrons with the same energy (cf. the tables in Bannikova & Kontorovich (2003a)) could possibly form the source image both in radio (due to synchrotron) and in X-ray bands (due to inverse Compton mechanism). As to the decametric band (Megn, Rashkovskiy & Shepelev, 2001) the observations in X-ray give the unique possibility to receive detailed information on the radiating electrons which is inaccessible from the radio sources.

Moreover the images of the sources in radio and X-ray bands differ from each other (see examples in Harris' list). For the jet of the quasar PKS 1136−135 (Sambruna et al., 2002) it is seen that the time-scale of the flares of radio and X-ray knots is of the same order. It means that the life time of radiating electrons also is of the same order. The radio image of the PKS 1136−135 jet is larger in size and not spatially coincident with the X-ray one. The reason for such a difference may

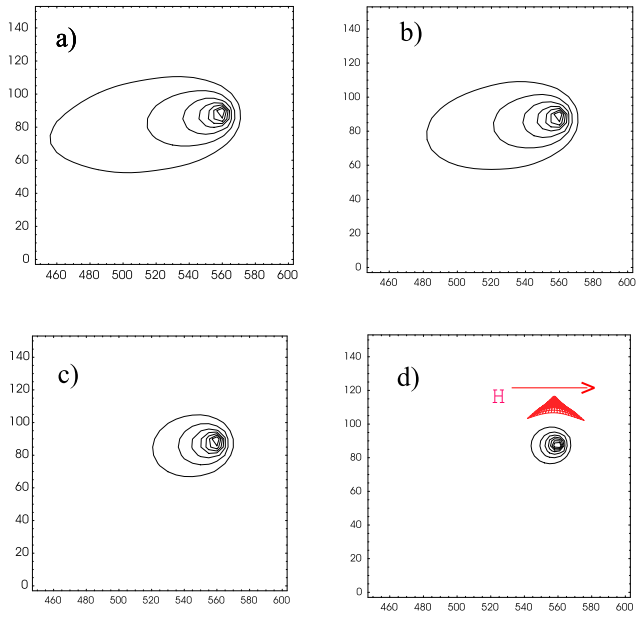

Figure 5: Model images of a flare for an uniform and exponentially decreasing magnetic field (red color) with H_0 = 10^{-7} G: a) the uniform field; b) r_0 = 740 pc; c) r_0 = 120 pc; d) r_0 = 30 pc.

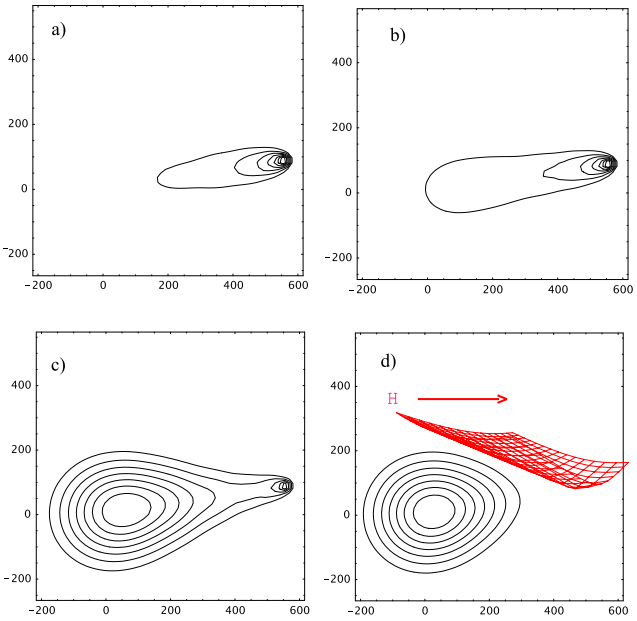

Figure 6: Model images of knot flares for a non-uniform asymmetric magnetic field increasing toward the edges (see Eq. (5)) (red color) with $H_0 = 10^{-8}$ G, $p = 2$, $h = 4$ for: a) r_0 = 900 pc; b) r_0 = 600 pc; c) r_0 = 300 pc; d) r_0 = 100 pc.

be the non-uniformity of the magnetic field[3]. We will discuss a similar situation (but not exactly as in PKS 1136−135) for the case when magnetic field is weak and electrons diffuse from the injection place having only pure Compton energy losses defined by the scattering on the space uniform relic radiation.

The magnetic field enters in the intensity expression in two ways. First, as a multiplier under the integral on the line of sight. Second, more complicated, through the link between the local value of the field and the energy of the electron radiating at the given frequency. In the inhomogeneous field the last dependence due to very non-uniform space distribution of electrons with given energy (see Fig. 3) could result in a sufficiently complicated isophote picture.

In this paper some variants of magnetic field dependence are shown (in all cases the field moves with the source) in Fig. 5, 6, 7:

1. The exponentially decreasing magnetic field is localized at the knot, $H(\mathbf{r}) = H_0 e^{-\rho/r_0}$, where $\rho = \sqrt{(V_x t - x)^2 + (V_y t - y)^2 + z^2}$ is the distance from the knot, r_0 is the characteristic scale of magnetic field non-homogeneity, and H_0 is its maximum value.

2. The magnetic field increases according to a power law, $H(\mathbf{r}) = H_0\,(\rho/r_0)^p$.

3. The asymmetric magnetic field increases toward the edges, axisymmetric with respect to the flare movement

$$H(\mathbf{r}) = H_0 \left[\left(1 - \left(\frac{\Theta}{\pi} \right)^2 \right)^h \left(\frac{\rho}{r_0} \right)^p + 1 \right], \qquad (5)$$

where $\Theta = \arctan[(V_y t - y)/(V_x t - x)]$.

The space non-uniform EDF forming radio band radiation on the given frequency $\nu = \nu_s$ in an inhomogeneous field $H(\mathbf{r})$ is shown in Fig. 3b. In each point electrons of different energies E radiate according to the condition $E \sim 1/\sqrt{H(\mathbf{r})}$. It is seen that the electrons with lower energies, the number of which is large, radiate in the regions of the stronger field. For a large distance from the injection point the number of electrons decreases due to the finiteness of their life time. The characteristic "two-hump" EDF (Fig. 3b) and isophote shape (Fig. 6c) are determined by both these effects.

[3]The other reasons are refraction of the radio image, heterogeneity of the radiation field giving the low-frequency quanta for inverse Compton process, or the thermal radiation of a hot (coronal) gas

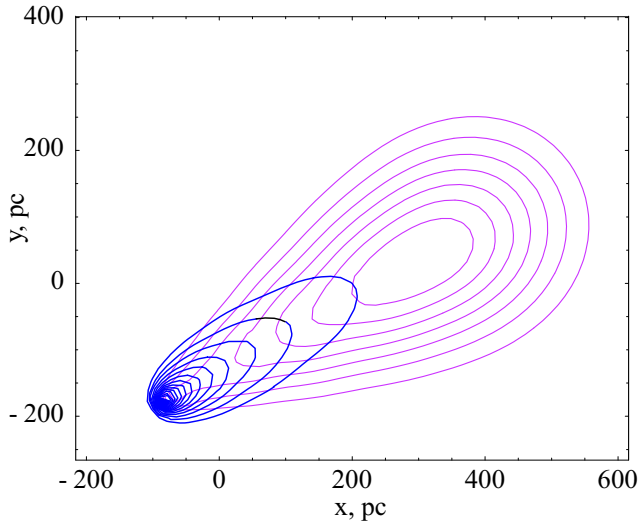

Figure 7: Model images of the same knot flares in radio (violet) and X-ray (blue). X-ray relates to the inverse Compton scattering on the relic radiation. Radio relates to the synchrotron radiation in the magnetic field, which increases with distance from the knot according to a power law with $H_0 = 10^{-8}$ G, $p = 1$, $r_0 = 100$ pc.

4 Summary

Radio galaxies and quasars are examined now with high angular resolution from radio to X-ray wavebands (Schwartz, 2003; Livio, 2003; Courvoisier, 2003; Hardcastle et al., 2002; Sambruna et al., 2002). We have shown that in the case of spatially uniform Compton losses on relic radiation we can solve the kinetic equation and find the distribution function of relativistic electrons analytically. In the frame of diffusion model of electron propagation from the local sources of their acceleration we can use this to investigate the shape of the knot flares as a function of physical parameters in the source. The difference between the images of jets of extragalactic sources in radio and X-ray bands, which are shaped by the same EDF due to subsequently synchrotron and Compton scattering mechanisms, gives us the possibility to obtain some additional information on magnetic field distribution in the sources.

Acknowledgments

The work is by part supported by the INTAS grant 00-00292.

References

Ginsburg, V. L. 1984, *"Astrophysics of Cosmic Rays"*, Moscow, Nauka, p. 360

Bannikova, E. Yu., Kontorovich, V. M. 2003, Space Science and Technology, 9, N5/6, 153

Courvoisier T. 2003, Gamma-ray and radio astronomy. In: JENAM 2003, Programm, Budapest, 22

Hardcastle, M. J. et al. 2002, astro-ph/0208204

Gestrin, S. G., Kontorovich, V. M., Kochanov, A. E. 1987, Kinem. Fiz. Neb. Tel., 3, N4, 57

Kolesnikov, F. M., Kontorovich, V. M. 2001, Radio Physics and Radio Astronomy, 6, N1, 32

Landau, L. D., Lifshits, E. M. 1988, Field Theory, Moscow, Nauka, p. 510

Livio M. 2003, Astrophysical Jets., In: JENAM 2003, Abstracts, Budapest, 157

Megn, A. V., Rashkovskiy, S. L., Shepelev, V. A. 2001, Radio Physics and Radio Astronomy, 6, N1, 9

Sambruna, R. M. et al. 2002, astro-ph/0201412

Schwartz, D. 2003, An X-ray of radio sources: the end of the story.In: JENAM 2003, Abstract, Budapest, 9

Valtaoja, E. 1982, A&A, 111, 213

Zheleznyakov, V. V. 1997, Radiation in Astrophysical Plasma, Moscow, "Janus-K", p. 528